

GALAXY GROUPS IN THE 2MASS REDSHIFT SURVEY

YI LU¹, XIAOHU YANG^{2,3}, FENG SHI¹, H.J. MO^{4,5}, DYLAN TWEED², HUIYUAN WANG⁶, YOUCAI ZHANG¹, SHIJIE LI¹, S.H. LIM⁴

Draft version June 16, 2019

ABSTRACT

A galaxy group catalog is constructed from the 2MASS Redshift Survey (2MRS) with the use of a halo-based group finder. The halo mass associated with a group is estimated using a ‘GAP’ method based on the luminosity of the central galaxy and its gap with other member galaxies. Tests using mock samples shows that this method is reliable, particularly for poor systems containing only a few members. On average 80% of all the groups have completeness > 0.8 , and about 65% of the groups have zero contamination. Halo masses are estimated with a typical uncertainty ~ 0.35 dex. The application of the group finder to the 2MRS gives 29,904 groups from a total of 43,246 galaxies at $z \leq 0.08$, with 5,286 groups having two or more members. Some basic properties of this group catalog is presented, and comparisons are made with other groups catalogs in overlap regions. With a depth to $z \sim 0.08$ and uniformly covering about 91% of the whole sky, this group catalog provides a useful data base to study galaxies in the local cosmic web, and to reconstruct the mass distribution in the local Universe.

Subject headings: large-scale structure of universe - dark matter - galaxies: halos - methods: statistical

1. INTRODUCTION

One important goal in modern cosmology is to establish the relationship between galaxies and dark matter halos in which galaxies form and reside. Understanding this galaxy-halo connection can provide important information about the underlying processes governing galaxy formation and evolution. Theoretically, there are several ways to study this relationship. The first is to use numerical simulations (Springel et al. 2005; Wadsley et al. 2004; Bryan et al. 1995; Kravtsov et al. 2002; Teyssier 2002; Springel 2010) or semi-analytical models (van den Bosch 2002; Kang et al. 2005; Croton et al. 2006). These approaches incorporate various physical processes that are potentially important for galaxy formation and evolution, such as gas cooling, star formation, feedback mechanisms, and so on. However, many processes in such modeling have to be approximated by sub-grid implementations and simple parameterizations, and so the results obtained are still questionable and sometimes fail to match observations. An alternative method to establish the galaxy-dark matter halo connection is to adopt an empirical approach. Models in this category includes the halo occupation model (e.g. Jing et al. 1998; Peacock et al. 2000; Berlind & Weinberg 2002; Zheng et al. 2005), the conditional luminosity functions (e.g. Yang, Mo & van den Bosch 2003; van den Bosch, Yang & Mo 2003; Yan, Madgwick & White 2003; Tinker 2005; Zheng et al. 2005; Cooray et al. 2006; van den Bosch et al. 2007; Yang et al. 2012), halo abundance matching (e.g. Mo et al. 1999; Vale & Ostriker 2004;

Conroy et al. 2006; Behroozi et al. 2010; Guo et al. 2010; Trujillo-Gomez et al. 2011), and parametric model fitting (Lu et al. 2014, 2015). By construction, the empirical approach can produce much better fits to the observational data than numerical simulations and semi-analytical models, and so the galaxy-halo relationship established in this way is more accurate. Yet another way of to establish the galaxy-dark matter halo connection is to identify galaxy systems (clusters and groups, collectively referred to as groups in the following) to represent dark halos. With a well-defined galaxy group catalog, one can not only study the relationship between halos and galaxies (e.g. Yang et al. 2005a, 2008; Lan et al. 2016; Erfanianfar et al. 2014; Rodríguez-Puebla et al. 2015; Jiang et al. 2016), but also investigate how dark matter halos trace the large-scale structure of the universe (e.g. Yang et al. 2005b; Yang et al. 2005c; Tal et al. 2014). In addition to these statistical studies, a well-defined group sample can also be used to reconstruct the current and initial cosmic density fields, so as to study not only the structures but also the formation histories of the cosmic web (e.g. Wang et al. 2012, 2013, 2014).

The quality of a group sample depends on the group finder used to identify individual groups. During the past two decades, numerous group catalogs have been constructed from various observations, including the 2-degree Field Galaxy Redshift Survey (2dFGRS) (Eke et al. 2004; Yang et al. 2005a), the DEEP2 survey (Crook et al. 2007) and the Sloan Digital Sky Survey (SDSS) (e.g. Berlind et al. 2006; Yang et al. 2007; Tago et al. 2010; Nurmi et al. 2013). The group finders adopted in these investigations range from the traditional friends-of-friends (FOF) algorithm (e.g. Davis et al. 1985), to the hybrid matched filter method (Kim et al. 2002) and the ‘‘MaxBCG’’ method (Koester et al. 2007). Although the accuracy of a particular group finder depends on the properties of the observational sample, all group finders need to handle the same observational effects, such as redshift distortion that impacts the clustering pattern of galaxies, and the variations of the mean inter-galaxy separation due to apparent magnitude limit.

In this paper, we present our construction of a galaxy group

¹ Key Laboratory for Research in Galaxies and Cosmology, Shanghai Astronomical Observatory, Nandan Road 80, Shanghai 200030, China; E-mail: luyi@shao.ac.cn

² Center for Astronomy and Astrophysics, Shanghai Jiao Tong University, Shanghai 200240, China; E-mail: xyang@sjtu.edu.cn

³ IFSA Collaborative Innovation Center, Shanghai Jiao Tong University, Shanghai 200240, China

⁴ Department of Astronomy, University of Massachusetts, Amherst MA 01003-9305, USA

⁵ Physics Department and Center for Astrophysics, Tsinghua University, Beijing 10084, China

⁶ Key Laboratory for Research in Galaxies and Cosmology, Department of Astronomy, University of Science and Technology of China, Hefei, Anhui 230026, China

catalog from the 2MASS Redshift Survey (2MRS), which is complete roughly to $K_s = 11.75$ and covers 91% of the sky (Huchra et al. 2012). Several group catalogs have already been constructed from 2MRS. Crook et al. (2007) constructed a group catalog using galaxies with a magnitude limit at $K_s = 11.25$ and a FOF algorithm similar to that of Huchra & Geller (1982). Tully (2015) built a group catalog in the volume between 3,000 and 10,000 km s^{-1} using a methodology similar to that of Yang et al. (2005a). Our goal here is to obtain a reliable and uniform galaxy group catalog using all galaxies in the 2MRS brighter than $K_s = 11.75$ to a redshift $z = 0.08$. In particular, we test the reliability of our catalog using realistic mock catalogs.

The group finder to be used is the halo-based group finder developed by Yang et al. (2005a), which groups galaxies within their host dark matter halos. This group finder is suitable to study the relation between galaxies and dark matter haloes over a wide range of halo masses, from rich clusters of galaxies to poor galaxy groups. It has been tested with mock galaxy surveys, and has been applied quite successfully to several galaxy catalogs (Yang et al. 2005a; Weinmann et al. 2006; Yang et al. 2007). The essential idea behind this group finder is to use the relationships between halo mass and its size and velocity dispersion when deciding the membership of a group. Thus an accurate estimate of the halo mass for a candidate galaxy group is a key step. As shown in Yang et al. (2007), for relative deep surveys, such as the SDSS, the group total luminosity (or stellar mass) provides a reliable ranking of the halo mass. In this case, halo masses can be estimated reliably by matching the rank of the characteristic luminosity of a group to that of halo mass given by a halo mass function. However, as pointed out in Lu et al. (2015), for a shallow survey, such as the 2MRS, where only a few bright member galaxies in a group can be observed, the characteristic group luminosity is no longer the best choice to estimate the halo mass. Instead, they proposed a method that is based on the luminosity of the central galaxy, L_c , and a luminosity ‘GAP’, L_{gap} , where the central galaxy is defined to be the brightest in a group, and the luminosity gap is defined as $\log L_{\text{gap}} = \log L_c - \log L_s$, with L_s being the luminosity of the satellite galaxy of some rank (e.g. the brightest, or second brightest satellite). The performance of the halo mass estimate is found to be enhanced by using the ‘GAP’ information. Comparisons between the true halo masses and the masses estimated with the ‘GAP’ method in mock catalogs show a typical dispersion of $\sim 0.3\text{dex}$.

In this paper, we modify the halo-based group finder developed by Yang et al. (2005a) by using the ‘GAP’ information. The structure of the paper is as follows. §2 describes the samples used in this paper, including the 2MRS galaxy sample and a mock galaxy sample used to evaluate the performance of our group finder. In §3 we describe our modified halo-based group finder. The performance of our group finder, including completeness, contamination, purity is discussed in §4, together with the reconstruction of the halo mass function. In §5 the properties of the group catalog constructed from 2MRS are detailed and compared to the mock group catalog, and to the SDSS DR7 galaxy group catalog constructed by Yang et al. (2007, 2012) in the overlapping region. Finally, we summarize our results in §6. Unless stated otherwise, we adopt a ΛCDM cosmology with parameters that are consistent with the nine-year data release of the WMAP mission (hereafter WMAP9 cosmology): $\Omega_m = 0.282$, $\Omega_\Lambda = 0.718$, $\Omega_b =$

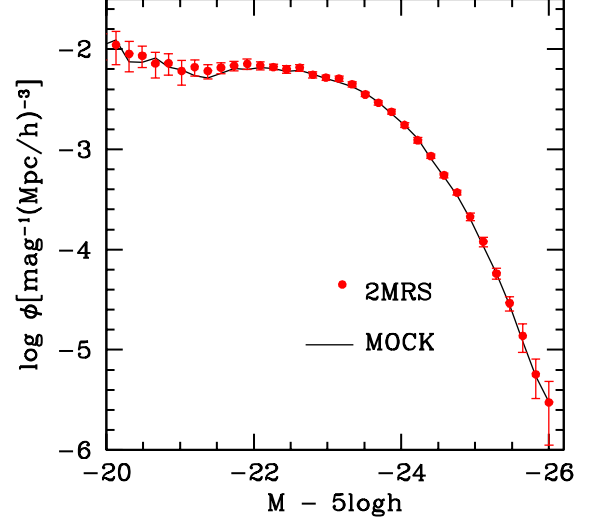


FIG. 1.— Luminosity functions in K_s band. Red points are obtained from the 2MRS galaxy sample, while black solid line represents the one obtained from the MOCK sample. The error bars are estimated using 1000 boot-strap re-sampling.

0.046 , $n_s = 0.965$, $h = H_0/(100 \text{ km s}^{-1} \text{ Mpc}^{-1}) = 0.697$ and $\sigma_8 = 0.817$ (Hinshaw et al. 2013).

2. DATA

2.1. The 2MRS galaxy catalog

The 2MASS Redshift Survey (2MRS) is based on the Two Micron All Sky Survey (Jarrett et al. 2000, 2003) and is complete to a limiting magnitude of $K_s = 11.75$, and $\sim 97.6\%$ of the galaxies brighter than the limiting magnitude have measured redshifts. The survey covers $\sim 91\%$ of the full sky; only $\sim 9\%$ of the sky close to the Milky Way plane is excluded (Huchra et al. 2012). The catalog contains about 43,533 galaxies extending out to $\sim 30,000 \text{ km s}^{-1}$. For our analysis we only use the 43,246 galaxies with $z \leq 0.08$. Among these, 25 entries have negative redshifts ($-0.001 \leq z < 0.0$) which are caused by the peculiar velocities of galaxies. In our analysis, all redshifts are corrected to the Local Group rest frame according to Karachentsev & Makarov (1996). We also use the distance information provided by Karachentsev et al. (2013) for some nearby galaxies, including 22 galaxies with negative redshifts in our 2MRS catalog, to reduce effects caused by peculiar velocities. Corrections of Virgo infall are made to 15 galaxies in the front and back of the Virgo cluster according to Karachentsev et al. (2014). Since the redshifts of our 2MRS galaxies are low, no attempt is made to apply any K - or E -corrections to galaxy luminosities.

From this catalog, we first measure the galaxy luminosity function (LF) in the K_s band. We adopt the commonly used $1/V_{\text{max}}$ algorithm (Schmidt 1968; Felten 1976), in which each galaxy is assigned a weight given by the maximum co-moving volume within which the galaxy could be observed. Fig 1 shows the galaxy luminosity function so obtained from our 2MRS sample, with the error bars estimated from 1,000 bootstrap re-samplings. We have fitted the LF to a Schechter function (Schechter 1976) and the best fit Schechter parameters are $\log \phi^* = 1.08e - 2$, $\alpha = -1.02$ and $M^* = -23.55$. These values are consistent with those obtained by Crook et al. (2007) and Tully (2015).

2.2. The mock 2MRS galaxy catalog

We construct a mock 2MRS galaxy catalog to test the performance of our group finder and the reliability of the final galaxy group catalog. The mock catalog is constructed as follows.

First, we use a high-resolution simulation carried out at the High Performance Computing Center, Shanghai Jiao Tong University, using L-GADGET, a memory-optimized version of GADGET-2 (Springel et al. 2005). A total of 3072^3 dark matter particles were followed in a periodic box of $500 h^{-1}\text{Mpc}$ on a side (Li et al. 2016). The adopted cosmological parameters are consistent with those from WMAP-9. Each particle in the simulation has a mass of $3.4 \times 10^8 h^{-1}\text{M}_\odot$. Dark matter halos were identified using the standard FOF algorithm (Davis et al. 1985) with a linking length of $b = 0.2$ times the mean inter particle separation.

Next, the halos are populated with galaxies of different luminosities. We use the conditional luminosity function (CLF, Yang, Mo & van den Bosch 2003), which is defined to be the average number of galaxies, as a function of luminosity, that reside in a halo of a given mass, to link galaxies with dark matter haloes. We make use of the set of CLF parameters provided by Cacciato et al. (2009) to generate model galaxies with r band luminosities. Following the observational definition, the central galaxy is defined as the brightest member and is assumed to be located at the center of the corresponding halo. Its velocity follows the velocity of the dark matter halo center. Other galaxies, referred to as satellite galaxies, are distributed spherically following a NFW (Navarro, Frenk & White 1997) profile. Their velocities are assumed to be the sum of the velocity of the host halo center plus a random velocity drawn from a Gaussian distribution with dispersion given by the virial velocity dispersion of the halo. We refer the reader to Lu et al. (2015) and Yang et al. (2004) for details.

In order to convert the r band magnitude to the K_s band, we first measure the *accumulative* luminosity function separately for both the mock and 2MRS samples. Assuming that galaxies more luminous in the r band are also more luminous in the K_s , we assign a K_s band luminosity (absolute magnitude) to each galaxy. In practice, we relate M_r and M_{K_s} through abundance matching:

$$\int_{-\infty}^{M_r} \phi_r(M'_r) dM'_r = \int_{-\infty}^{M_{K_s}} \phi_{K_s}(M'_{K_s}) dM'_{K_s}, \quad (1)$$

where $\phi_r(M_r)$ and $\phi_{K_s}(M_{K_s})$ are the luminosity functions of galaxies in M_r and M_{K_s} , respectively.

Finally, we place a virtual observer at the center of our simulation box and define a (α, δ) -coordinate frame, and remove all galaxies that are located outside the survey region ($\sim 9\%$ of the total sky). We then assign to each galaxy a redshift and an apparent magnitude according to its distance and luminosity, and select only galaxies that are brighter than the magnitude limit $K_s = 11.75$. Here again, no K+E corrections are made to galaxy luminosities. In total, we have 41,876 galaxies in our mock 2MRS catalog. The black solid curve in Fig. 1 shows the K_s band luminosity function estimated from our mock sample.

Since we have both the true halo mass and the galaxy membership informations in our mock sample, we can use it to test the performance of our group finder. Hereafter, we refer to results obtained from 2MRS and mock 2MRS samples as ‘2MRS’ and ‘MOCK’ respectively. Sub-samples with true

TABLE 1
COMPARISON BETWEEN THREE SAMPLES

Sample	Parent Catalog	Group Finder	Halo Mass
2MRS	2MRS catalog	halo-based	Gap model
MOCK	2MRS mock catalog	halo-based	Gap model
TRUE	2MRS mock catalog	None	true halo mass

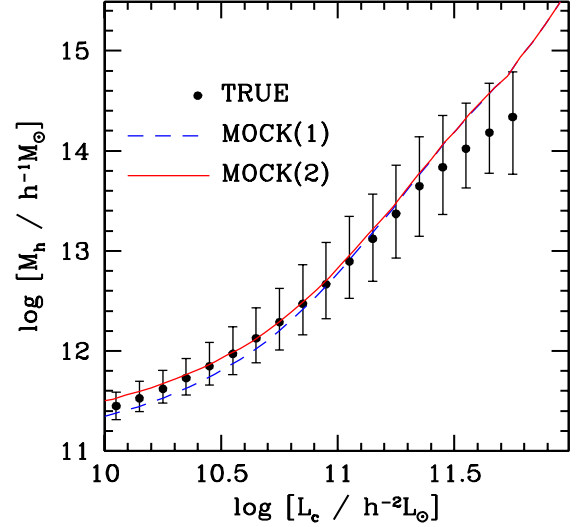


FIG. 2.— $L_c - M_h$ relation given by the mock sample using abundance matching between the accumulative luminosity function of galaxies and the halo mass function. ‘Round 1’ relation is obtained using all mock galaxies [blue dashed line, labelled MOCK(1)] while ‘Round 2’ is obtained using central galaxies only [red line labelled MOCK(2)]. The intrinsic $L_c - M_h$ relation given by the mock sample itself is plotted with black solid points with error bars which indicate the 68% confidence level around the median.

halo masses and memberships are referred to as ‘TRUE’. For clarity, we list the differences of the three definitions in Table. 1, including the group finders that were used to identify groups, and the methods used to estimate the halo masses.

3. THE MODIFIED HALO-BASED GROUP FINDER

One of the key steps in the halo-based group finder (Yang et al. 2005a, 2007) is to have accurate estimates of the halo masses of candidate galaxy groups. As demonstrated in Yang et al. (2007), halo mass is tightly correlated with the total luminosity of member galaxies. In practice, however, one can only estimate a characteristic luminosity which is the sum of the luminosities of member galaxies brighter than some given limit. For a relatively deep survey such as the SDSS, where the limit can be set sufficiently low, the characteristic luminosity is a good proxy of the total luminosity and so can be used to indicate halo mass. For a shallow survey like the 2MRS, on the other hand, only a few (in most cases one or two) brightest member galaxies in the halos can be observed. The characteristic luminosity is no longer the best halo mass estimator, and an alternative is needed. In this paper, we implement the ‘GAP’ method proposed by Lu et al. (2015).

3.1. The GAP halo mass estimator

In the ‘GAP’ method, one first needs to estimate the $L_c - M_h$ relation. In general one can obtain this relation from the conditional luminosity function model (e.g. Yang, Mo & van den Bosch 2003) or from halo abun-

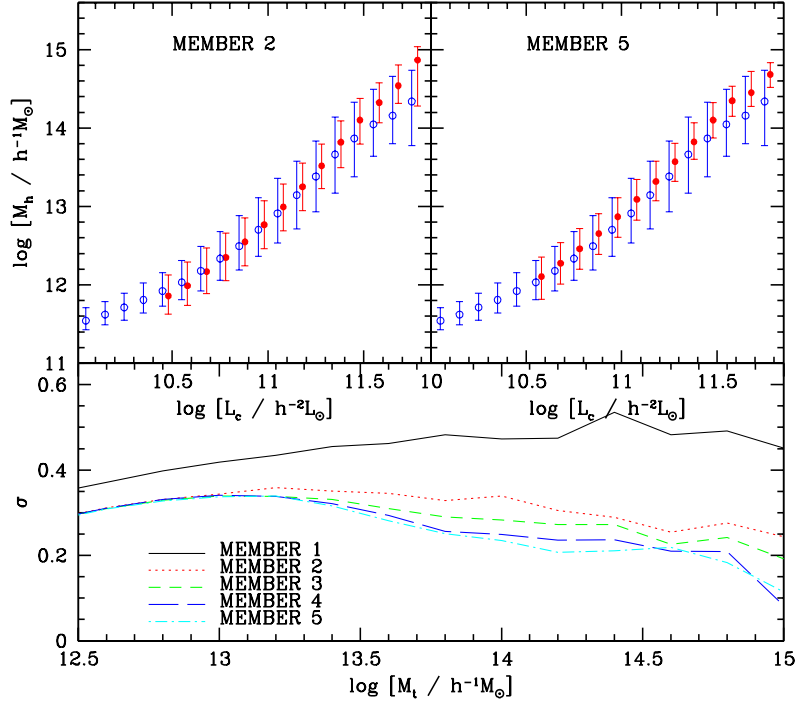


FIG. 3.— Comparison between the original (open blue circles) $\log M_h$ and corrected (solid circles) $\log M'_h$ halo masses by using the luminosity gap between the central (brightest) and the second brightest (top left) and the fifth brightest member galaxies (top right), respectively. The standard variances σ between estimated halo mass and the true halo mass are illustrated in the bottom panel. As the legend indicates, results are shown for groups with 2, 3, 4 and 5 members, while the halo masses estimated only by using central galaxies (member 1) are also given in the same panel.

TABLE 2
PARAMETERS OF THE $\Delta \log M_h$ MODEL OBTAINED FROM MOCK. [SEE EQS. (4) & (5)]

$\Delta \log M_h$	β_1	α_2	β_2	β_3	γ_3
MEMBER 2	$10.81^{+0.18}_{-0.19}$	$0.36^{+1.60}_{-0.26}$	$-15.44^{+3.35}_{-7.86}$	$10.39^{+0.11}_{-0.24}$	$1.94^{+0.83}_{-0.41}$
MEMBER 3	$10.21^{+0.39}_{-0.10}$	$0.23^{+0.54}_{-0.14}$	$-13.40^{+1.21}_{-3.97}$	$9.90^{+0.36}_{-0.10}$	$2.21^{+0.32}_{-0.27}$
MEMBER 4	$9.98^{+0.32}_{-0.18}$	$0.20^{+0.25}_{-0.09}$	$-13.39^{+1.10}_{-2.76}$	$9.81^{+0.30}_{-0.17}$	$2.45^{+0.24}_{-0.15}$
MEMBER 5	$9.77^{+0.33}_{-0.07}$	$0.13^{+0.15}_{-0.01}$	$-13.67^{+1.18}_{-0.94}$	$9.67^{+0.28}_{-0.07}$	$2.54^{+0.15}_{-0.08}$

dance matching (e.g. Mo et al. 1999; Vale & Ostriker 2006; Conroy et al. 2006; Behroozi et al. 2010; Guo et al. 2010). Here we adopt the latter and assume that there is a monotonic relation between the luminosity of central galaxy and the mass of dark matter halo, so that a more luminous galaxy resides a more massive halo. We can then get an initial estimate of the dark matter halo mass for each central galaxy from

$$\int_{L_c}^{\infty} n_c(L'_c) dL'_c = \int_{M_h}^{\infty} n_h(M'_h) dM'_h, \quad (2)$$

where, $n_c(L_c)$ is the number density of central galaxies with luminosity L_c and $n_h(M_h)$ is the number density of halos with mass M_h . Note that, in this abundance matching approach, we need to know whether a galaxy is a central or a satellite. Since we are trying to find galaxy groups within the observation (the 2MRS in our case), we can easily separate galaxies into centrals and satellites with the help of group

memberships. As we will show later, although the L_c - M_h relation we obtain may deviates from the true one, especially at the massive end, the deviation can be compensated to some extent by our ‘GAP’-based correction factor.

Our modeling of the L_c - M_h relation using Eq. (2) is carried out via the following two steps. First, before we are able to separate galaxies into centrals and satellites with the help of group memberships, we assume that all of them are centrals (as shown in Yang et al. 2008, more than 60% of the galaxies are centrals). We have applied this to our mock 2MRS sample, and obtain the ‘Round 1’ L_c - M_h relation, which is shown in Fig. 2 as the blue dashed line.

For comparison, we also plot, as black solid points, the real L_c - M_h relation obtained from the TRUE groups with error bars indicating the 68% confidence level around the median values. Compared to the TRUE relation, we see that, the Round 1 relationship shows a general agreement with the

TRUE, with a slight over-prediction of the halo masses at the bright end and slight under-prediction at the faint end. The deviation at the massive end is caused by the Malmquist bias in the L_c - M_h relation which can be corrected by the ‘GAP’ (see Lu et al. 2015). The deviation at the faint end is caused by the inclusion of all the galaxies (including satellites) in our abundance matching. As we apply our group finder to the galaxy catalog in the next step, the group membership will enable us to separate galaxies into centrals and satellites. We can then limit the application of the abundance matching to centrals only, and improve the L_c - M_h relation. After two to three iterations we converge to a new set of group memberships and a new L_c - M_h relationship, which is referred to as ‘Round 2’ and shown as the solid red line in Fig. 2. After this step, there is no longer any systematic deviation of the L_c - M_h relationship relative to the TRUE at the low mass end.

With the L_c - M_h obtained in this step, we can estimate the ‘luminosity gap’, which is defined as the luminosity ratio between the central and a satellite galaxy in the same halo, $\log L_{\text{gap}} = \log(L_c/L_s)$ Lu et al. (2015). The halo mass is then estimated using the relation,

$$\log M_h(L_c, L_{\text{gap}}) = \log M_h(L_c) + \Delta \log M_h(L_c, L_{\text{gap}}). \quad (3)$$

This halo mass estimator consists of two parts. The first term on the right side is an empirical relation between M_h and L_c , derived from Eq. (2). The second term, $\Delta \log M_h(L_c, L_{\text{gap}})$, represents the amount of correction to that relation. We use the following functional form to model this term of correction,

$$\Delta \log M_h(L_c, L_{\text{gap}}) = \eta_a \exp(\eta_b \log L_{\text{gap}}) + \eta_c. \quad (4)$$

The parameters η_a , η_b and η_c all depend on L_c as:

$$\begin{aligned} \eta_a(L_c) &= \exp(\log L_c - \beta_1) \\ \eta_b(L_c) &= \alpha_2(\log L_c + \beta_2) \\ \eta_c(L_c) &= -(\log L_c - \beta_3)^{\gamma_3} \end{aligned} \quad (5)$$

which is specified by five free parameters.

For a given L_c - M_h relation derived from Eq. 2 (Round 1 or Round 2), we fit the model to the true halo masses for our galaxy systems (groups) in our mock 2MRS (see Lu et al. 2015, for details). Table 2 presents the set of best fit values of these parameters. Since the 2MRS sample is shallow, we provide the parameters up to 5 group members. As an illustration, Fig. 3 shows the performance of this halo mass estimator. In the top two panels, the original $\log M_h(L_c)$ relations are shown as the open circles; the GAP-corrected relations are shown as the solid points, with the left panel showing results for $L_s = L_2$ and the right for $L_s = L_5$. It is clear that the scatter in $\log M'_h(L_c)$ is significantly reduced relative to the original relation, especially for massive halos/groups, where the scatter is reduced by a factor of about two. The bottom panel of Fig. 3 shows the standard deviation σ of the halo mass $\log M_h(L_c, L_{\text{gap}})$ obtained by Eq.(3) from the true halo mass $\log M_t$. In both Lu et al. (2015) and this paper, we find that using L_5 gives the best correction to the halo mass. As shown Lu et al. (2015), such a correction factor is quite independent of the galaxy formation model used to construct the mock catalog. In this paper we use the set of best fit parameters only up to the fifth ranked member (see below).

3.2. The Group Finder

The group finder adopted here is similar to that developed by Yang et al. (2005a). It uses the general properties of dark

matter haloes, namely size and velocity dispersion, to iteratively find galaxy groups. Tests show that this group finder is powerful in linking galaxies with dark matter halos, even in the case of single member groups. As we pointed out earlier, the halo mass estimation adopted in Yang et al. (2005a, 2007) is based on the ranking of the characteristic group luminosity and proves to be quite reliable for surveys like the 2dFGRS and SDSS. For the 2MRS considered here, we use the ‘GAP’-corrected estimator described above. The modified group finder with this halo mass estimator consists of the following main steps:

Step 1: Start the halo-based group finder.

In the earlier version of the halo-based group finder, the first step is to use the FOF algorithm (Davis et al. 1985) with very small linking lengths in redshift space to find potential groups. Here we assume all galaxies in our catalog are candidate groups. The halo mass of each candidate group is calculated using the $L_c - M_h$ relation obtained in Eq. (2) (Round 1).

Step 2: Update group memberships using halo information.

After assigning halo masses to all the candidates, groups are sorted according to their halo masses. Starting from the most massive one, we estimate the size and velocity dispersion of the dark matter halo, using the halo mass currently assigned to it. A dark matter halo is defined to have an over-density of 180. For the WMAP9 cosmology adopted here, the radius is approximately

$$r_{180} = 1.33 h^{-1} \text{Mpc} \left(\frac{M_h}{10^{14} h^{-1} \text{M}_{\odot}} \right)^{1/3} (1 + z_{\text{group}})^{-1}, \quad (6)$$

where z_{group} is the redshift of the group center. The line-of-sight velocity dispersion of the halo is

$$\sigma = 418 \text{ km s}^{-1} \left(\frac{M_h}{10^{14} h^{-1} \text{M}_{\odot}} \right)^{0.3367}. \quad (7)$$

Finally, following Yang et al. (2007, hereafter Y07), we use the luminosity weighted center of member galaxies as the new group center.

Once we have a tentative group center and tentative estimates of halo size and velocity dispersion, we can assign new galaxies to the group. We assume that the phase-space distribution of galaxies follows that of dark matter. The number density of galaxies in the redshift space around the group center (assumed to coincide with the center of halo) at redshift z_{group} can then be written as a function of the projected distance R and $\Delta z = z - z_{\text{group}}$:

$$P_M(R, \Delta z) = \frac{H_0}{c} \frac{\Sigma(R)}{\bar{\rho}} p(\Delta z), \quad (8)$$

where c is the speed of light and $\bar{\rho}$ is the average density of the Universe. The projected surface density, $\Sigma(R)$, is assumed to be that given by a (spherical) NFW (Navarro, Frenk & White 1997) profile:

$$\Sigma(R) = 2 r_s \bar{\delta} \bar{\rho} f(R/r_s), \quad (9)$$

where r_s is the scale radius, and the shape function is

$$f(x) = \begin{cases} \frac{1}{x^2-1} \left(1 - \frac{\ln \frac{1+\sqrt{1-x^2}}{\sqrt{1-x^2}}}{\sqrt{1-x^2}} \right) & \text{if } x < 1 \\ \frac{1}{3} & \text{if } x = 1 \\ \frac{1}{x^2-1} \left(1 - \frac{\text{atan}\sqrt{x^2-1}}{\sqrt{x^2-1}} \right) & \text{if } x > 1 \end{cases} \quad (10)$$

The normalization of the profile depends on the concentration $c_{180} = r_{180}/r_s$ as:

$$\bar{\delta} = \frac{180}{3} \frac{c_{180}^3}{\ln(1 + c_{180}) - c_{180}/(1 + c_{180})}. \quad (11)$$

The function $p(\Delta z)d\Delta z$ describes the redshift distribution of galaxies within the halo, and is assumed to have the normal distribution,

$$p(\Delta z) = \frac{1}{\sqrt{2\pi}} \frac{c}{\sigma(1 + z_{\text{group}})} \exp \left[\frac{-(c\Delta z)^2}{2\sigma^2(1 + z_{\text{group}})^2} \right], \quad (12)$$

where σ is the rest-frame velocity dispersion given by equation (7). So defined, $P_M(R, \Delta z)$ is the three-dimensional density in redshift space. In order to assign a galaxy to a particular group we proceed as follows. For each galaxy we loop over all groups, and compute the distances R and Δz between the galaxy and the group center. An appropriately chosen background level (see Yang et al. 2005a) $B = 10$ is applied to the density contrast for galaxies to be assigned to a group. If, according to this criterion, a galaxy can be assigned to more than one group it is only assigned to the one with the highest $P_M(R, \Delta z)$. Finally, if all members of two groups can be assigned to one, they are merged into a single group.

Step 3: Update halo mass with ‘GAP’ correction.

Once the new membership to a group is obtained, we use the new central and satellite galaxy system to estimate the halo mass using the ‘GAP’ method described by Eq. (3). For each candidate group, we use the L_c - M_h relation and the luminosity gap $\log L_{\text{gap}}$ between the central galaxy and the faintest satellite (if the group contains less than 5 members) or the fifth brightest galaxy (if the group has membership equal to or larger than 5), to estimate the halo mass. In practice, we only apply the luminosity gap correction for centrals in the luminosity range $10.5 \leq \log L_c \leq 11.7$. As shown in the top panels of Fig. 3, fainter ($\log L_c \leq 10.5$) central galaxies are basically isolated. For $\log L_c \geq 11.7$, we found that using the value of L_c directly in the GAP leads to over-correlation. Thus, for these systems we set $\log L_c = 11.7$ to estimate the GAP correction. In addition, since our galaxy sample is magnitude limited to $K_s = 11.75$, our method also suffers from a ‘missing satellite’ problem, in that some groups do not contain any satellites brighter than the magnitude limit. As an attempt to partly correct for this, we assume that each galaxy group that contains only one member (a central) has a potential member satellite galaxy with an apparent magnitude $K_s = 11.75$, which corresponds to a limiting luminosity L_{limit} at the distance of the group. A ‘GAP’ correction, $\log L_c - \log L_{\text{limit}}$, is also applied to all groups of single membership with $\log L_c - \log L_{\text{limit}} \geq 0.5$, and the final halo mass of such a group is set to be the average value between this mass and the original mass based on the central galaxy alone.

Step 4: Update the L_c - M_h relation and Iterate.

Once all the groups have been updated for new memberships, we can distinguish between centrals and satellites. We use the updated central galaxy sample to update the L_c - M_h relation (Round 2) to be used to assign halo masses to tentative groups. We iterate Steps 2-4 until convergence is reached. Typically three iterations are needed to achieve convergence. Our final catalog is the collection of all the converged groups with information about their positions, galaxy memberships, and halo masses.

Step 5: Update the final halo masses of groups.

Once all the groups (memberships) have been finalized, we perform a final update of the halo masses of groups using an abundance matching method so that the halo mass function of the groups is consistent with theoretical predictions (e.g. Yang et al. 2007).

In order to make the abundance matching, one needs to have a complete sample of groups (halos), i.e. to obtain the limiting redshift for a given mass of halos, within which the selection of groups is complete. Unlike the luminosity for which the limiting redshift can be directly calculated from the magnitude limit, we use an empirical way to get the limiting redshift for halos. As an illustration, we use the TRUE masses of halos in the mock 2MRS catalog to obtain such a limiting redshift as a function of halo mass. First, we calculate the number densities of halos in small redshift and mass bins and plot them in the $\log M_h$ - z plane using color bars (see Fig. 4). We can see that the number density of halos of given mass drops sharply above certain redshift. Here we define the limiting redshift for a given mass halos as the redshift at which this rapid drop in density occurs. The smooth line in Fig. 4 shows the limiting redshift as a function of $\log M_h$ we use, which clearly represents a conservative cut to ensure completeness. Once a limiting redshift is adopted, we can calculate the halo mass function using only halos below this redshift. Fig. 5 shows the halo mass function obtained in this way with dots and error bars). Here again, the error bars are estimated using 1000 bootstrap re-samplings. For comparison, we also show, using the solid line, the theoretical model predictions given by Tinker et al. (2008). Compared with the model prediction, the data points are slightly lower at intermediate to low mass range, which we believe is mainly due to cosmic variance.

Once the GAP halo masses for all the groups are obtained, we measure the *accumulative* halo mass function using the procedures described above. The measurement is then matched with the theoretical halo mass function. Finally, the differences between the GAP mass and the model mass is then applied to all the groups of a given GAP mass.

4. TEST WITH MOCK CATALOGS

In this section, we test the performances of our group finder, both in halo masses and group memberships it assigns, by comparing the groups selected by our group finder with the ‘TRUE’ groups in our mock 2MRS.

4.1. Completeness, Contamination and Purity

Starting from a total of 43,246 galaxies in the 2MRS, our group finder returns 29,904 galaxy groups, among which 5,286 have 2 or more members, and the rest only one member. To assess the performance of the group finder we follow Yang et al. (2005a, 2007) and proceed as follows. For each

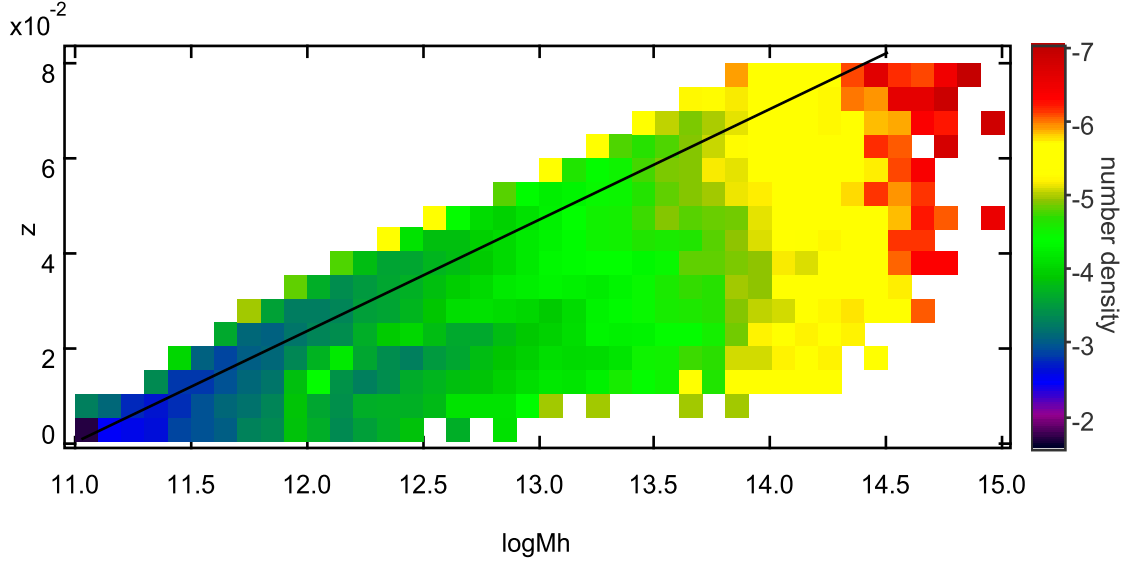


FIG. 4.— The number densities of halos, $\log \phi[(h^{-1}\text{Mpc})^{-3}]$, in each halo mass and redshift bins shown with color bars. The solid line represents a conservative redshift limit $z_{\text{limit}} = 0.023 * \log M_h - 0.26$, below which a complete sample can be formed for halos with masses down to the mass given by the value of M_h shown by the horizontal axis.

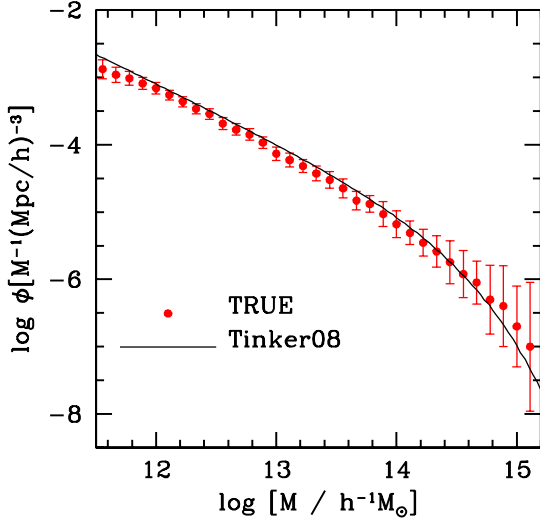


FIG. 5.— The halo mass function of our TRUE sample (dots with error bars). The halo mass function given by Tinker et al. (2008) is also plotted in the same panel for comparison using black solid line.

group k , we identify the halo ID, h_k , of its brightest member. We define N_t to be the total number of true members in the mock sample that belong to halo h_k , N_s to be the number of true members that our group finder has identified as members of group k , N_i to be the number of interlopers (group members that belong to a different halo), and N_g to be the total number of group members selected. Using these numbers, we define the following three quantities:

- COMPLETENESS: $f_c \equiv N_s/N_t$;
- CONTAMINATION: $f_i \equiv N_i/N_t$;
- PURITY: $f_p \equiv N_t/N_g$.

Since $N_g = N_i + N_s$, we have that $f_p = 1/(f_c + f_i)$. A PURITY $f_p < 1$ implies that the number of interlopers is larger than the number of missed true members, while $f_p > 1$ implies that the group is incomplete ($f_c < 1$) and the number of missed true members is larger than the number of interlopers. Note that the identification of the halo hosting a group is solely based on the halo ID of the brightest galaxy member. Consequently, the contamination f_i can be larger than unity. A perfect group finder yields groups with $f_c = f_p = 1$ and $f_i = 0$. Note also that the value for the background level $B = 10$ was tuned to maximize the average value of $f_c(1 - f_i)$, as described in Yang et al. (2005a).

Fig. 6 shows the results obtained from the mock 2MRS galaxy and group samples. Following Y07, here results are only shown for groups with richness $N \geq 2$, since groups with a single member have zero contamination ($f_i = 0$) by definition. The upper left panel shows the cumulative distributions of the COMPLETENESS f_c . Different lines correspond to groups of different true halo masses, as indicated. The fraction of groups with 100 percent completeness ($f_c = 1$) depends on halo mass, and ranges from $\sim 85\%$ for low-mass groups to $\sim 65\%$ for the most massive ones. Since the group finder in this paper is aimed to maximize the average value of $f_c(1 - f_i)$, massive groups with larger velocity dispersions have larger f_i due to contamination of foreground and background galaxies. A compromise between f_c and f_i leads to smaller f_c for more massive groups. We see that more than 90% of all groups have COMPLETENESS $f_c > 0.6$. For groups with $\log M_h \leq 14$, about 80% of all groups have $f_c > 0.8$; only for massive halos with $\log M_h > 14$ is this fraction a little lower, $\sim 75 - 80\%$.

The middle left panel of Fig. 6 shows the cumulative distribution of the CONTAMINATION f_i . The fraction of groups with $f_i = 0$ ranges from 60% to 80%, depending on the halo mass, while $\sim 85\%$ of all the groups have $f_i < 0.5$. The interlopers producing the contamination are either nearby field galaxies or the member galaxies of nearby massive groups, es-

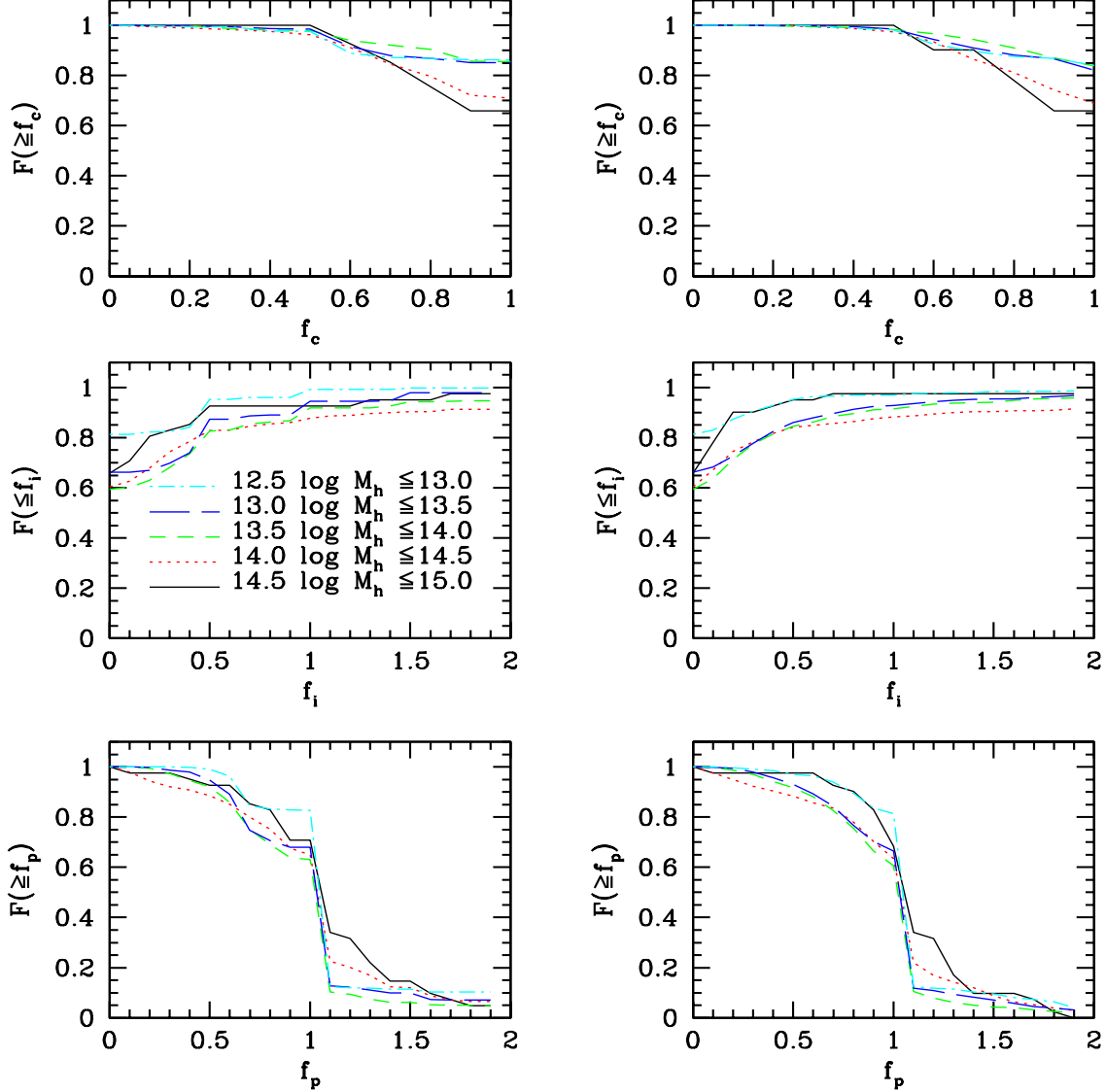


FIG. 6.— The top, middle and bottom panels show the cumulative distributions of completeness, f_c (the fraction of true members), contamination, f_i (the fraction of interlopers), and purity, f_p (ratio between the the number of true members and the total number of group members). These values are number weighted in the left panels and luminosity weighted in the right panels. Different lines represent the results for groups in halos of different masses, as indicated. Results are plotted for groups with at least 2 members, since groups with only 1 member have, by definition, $f_i = 0$.

pecially for systems that are along the same line of sight. Although the results for different halo masses are similar, groups in the lowest mass bin seems to have the highest fraction of interlopers.

Finally, the lower left panel shows the cumulative distribution of the PURITY f_p . We see that there are on average as many groups with $f_p < 1$ as with $f_p > 1$. The break at $f_p = 1$ indicates that the number of recovered group members is about the same as the number of the true members. Thus, the sharper the break is, the better, and the ideal case is a step function at $f_p = 1$. As one can see, only for massive haloes there is a small fraction, $\sim 10\%$, with $f_p < 0.5$, and a significant fraction, $\sim 15\%$, with $f_p > 1.5$.

Following Y07, we also describe the completeness, contamination and purity in terms of the total luminosity rather than the number of member galaxies. The corresponding results are shown in the three right panels of Fig. 6, respectively.

These results are very similar to those in terms of the number of member galaxies shown in the left panels.

We now turn to the global properties of groups. We first examine the *global completeness*, f_{halo} , defined to be the fraction of halos in the mock catalog whose brightest members have actually been identified as the brightest (central) galaxies of the corresponding groups. The left panel of Fig. 7 shows f_{halo} as a function of the true halo mass, obtained from our MOCK sample for halos with $N_t \geq 1$ (solid blue line) and $N_t \geq 3$ (dashed red line), respectively. As one can see, the group finder successfully selects more than 90% of all the true halos with masses $\geq 10^{13} h^{-1} M_\odot$, almost independent of their richness. The large fluctuations in the red dashed line at the low-mass end is due to the small number of groups in the corresponding sample. There is a weak trend with halo mass, in the sense that the performance of the group finder, in terms of f_{halo} , is better for more massive halos. The other global

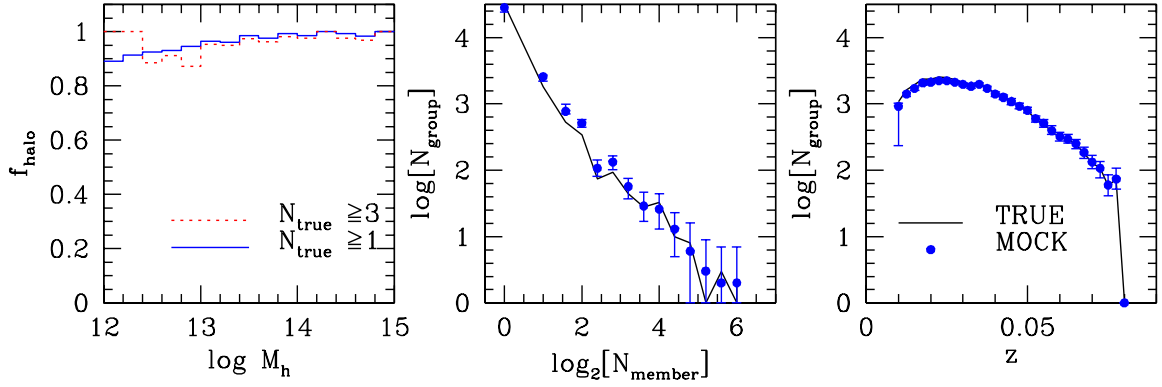


FIG. 7.— Left panel: global completeness f_{halo} , defined as the fraction of halos in the mock sample whose brightest member has actually been identified as the brightest (central) galaxy of its group, as function of the true halo mass M_h . Results are shown for all halos (solid blue line) and for those with at least three members in the mock sample (dashed red line). Middle and right panels: the distributions of richness (middle) and redshift (right) of groups. The results obtained from the group catalog constructed from the mock galaxy sample are represented by solid points. The error bars are estimated from 1000 bootstrap re-samplings. The distributions obtained from TRUE are shown by the solid lines.

properties we examined are the richness and redshift distributions of galaxy groups. Shown in the middle and right panel of Fig. 7 are the two resulting distributions for the MOCK and TRUE samples, respectively, and good agreement is clearly seen between MOCK and TRUE.

4.2. Halo masses of galaxy groups

An important aspect of our group finder is the assignment of halo masses to the groups. An accurate halo mass estimate is not only important in determining group memberships according to common dark halos, but also in the applications of our group catalog to the investigations of galaxy populations in halos and large-scale structure traced by galaxy groups. As described above, our halo mass estimate is based on the ranking of the ‘GAP’ corrected luminosities of central galaxies, and our test in §3.1 using TRUE halo masses and group membership information shows that this halo mass estimate is unbiased and has scatter typically of 0.35 to 0.2 dex for halos with masses between $\sim 10^{13}$ to $\sim 10^{15} h^{-1} M_\odot$. However, in real applications, the halo mass estimate also suffers from survey selection effects, contamination and incompleteness of group memberships, and so on. The accuracy of the mass estimate is expected to be reduced. Here we check the accuracy of our halo mass estimates using groups selected from our mock 2MRS with the use of our group finder.

Fig. 8 shows the comparison between the true halo mass M_t and the estimated halo mass M_h from the mock 2MRS group catalog. A MOCK group is paired with a TRUE if both contains the same central galaxy, and we compare the halo mass assigned to the MOCK group by our group finder with the TRUE halo mass. The left panel of Fig. 8 shows the comparison for all groups while the right panels for MOCK groups with more than one member. The corresponding standard deviations are plotted in the bottom two panels, with different lines representing groups of different richness. Fig. 8 shows that the deviation is typically between 0.2 - 0.45 dex for all groups, with some dependence on halo mass. For $N \geq 1$, the scatter appears to be the largest for halos with $M_t \sim 10^{13} h^{-1} M_\odot$. The bottom right panel shows that the mass estimate is improved as the group richness increases. For groups with $N \geq 3$, the scatter is about 0.35 dex, which is comparable to that obtained by Y07 for SDSS groups.

The halo mass function recovered is another important test of the group finder. In Fig. 9 we show, as the solid points with error bars (obtained by 1000 bootstrap re-samplings), the halo mass function obtained from our mock 2MRS groups selected by our group finder. For comparison, the true halo mass function is shown as the solid line. Note that, here we have not applied any corrections for incompleteness to both MOCK and TRUE samples. We see that the halo mass function obtained with our group finder matches fairly well with the true mass function. The slight over prediction of the halo mass function at the intermediate mass range in the MOCK is caused by the fact that we have forced the final halo mass function of groups to agree with theoretical model prediction, while the real mass function of TRUE may deviate from the theoretical prediction due to cosmic variance.

5. THE 2MRS GALAXY GROUP CATALOG

We apply our modified group finder to the 2MRS galaxy catalog in exactly the same way as described in the last section. In the following, we describe our catalog and present some of its basic properties. We also make comparisons with the SDSS groups in the overlapping region, and discuss how some known nearby structures are represented in our catalog.

5.1. Basic Properties

Our modified halo-based group finder identifies 29,904 groups from a total of 43,246 2MRS galaxies in the redshift range $z \leq 0.08$. Among the groups selected, 5,286 have two or more members; 2,208 are triplets; and 1,189 have four or more members. Fig. 11 shows the distribution of all groups in the 2MRS catalog. In the upper panel, the red points represent groups in the redshift range $0.0 < z \leq 0.02$, while green and blue points represent groups in $0.02 < z \leq 0.03$ and $0.03 < z \leq 0.08$, respectively. In the lower panel, red, green and blue points represent groups in mass ranges $\log M_h \geq 13.5$, $13.5 \geq \log M_h \geq 12.5$ and $12.5 \geq \log M_h$, respectively. One can see from the lower panel that more massive groups seem to locate preferentially denser regions. In addition to the sky projection, we also show two slices of the distribution from the North and South hemisphere near the galactic equatorial with thickness $10 \leq b < 20$ and $-20 \leq b < -10$, respectively. The corresponding results

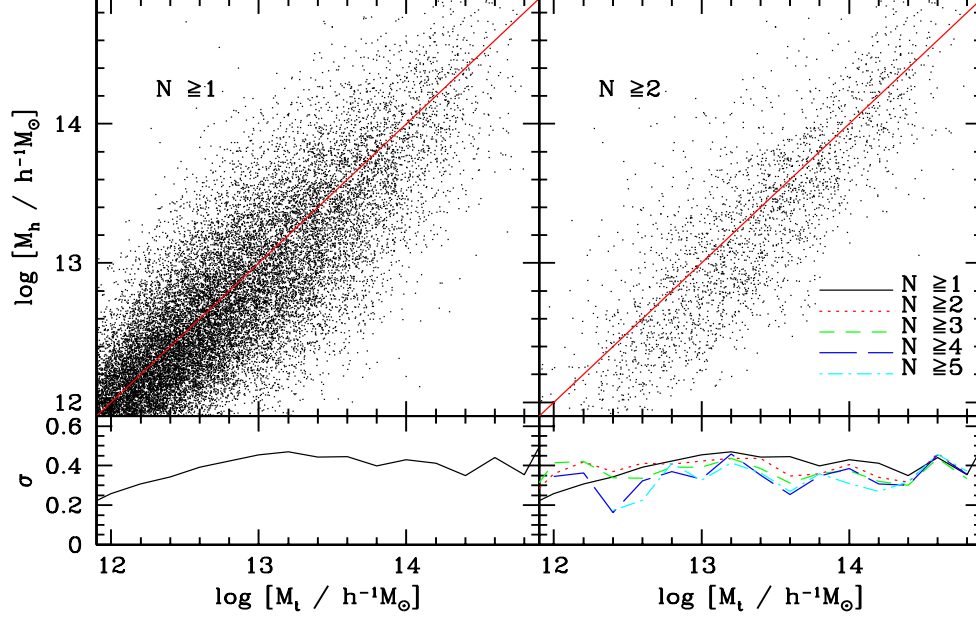


FIG. 8.— Comparison between the estimated halo mass M_h by group finder and the true halo mass M_t given by the mock sample. Points in top panels are shown for all groups (left) and groups with more than one members (right). Red lines show the relation $M_h = M_t$. The standard variations from the red lines are shown as σ in the bottom small panels, with different lines represent results for groups with different richness, as indicated.

TABLE 3
PROPERTIES OF 2MRS CATALOGS

Sample	Galaxies	Groups	$N = 1$	$N \geq 2$	$14.0 \geq \log M_h \geq 13.0$	$\log M_h \geq 14.0$
2MRS $0.01 \leq z \leq 0.03$	20921	12879	10004	2875	1495	61
2MRS $0.0 \leq z \leq 0.08$	43246	29904	24617	5286	8484	1103
MOCK	41876	32368	23531	4817	8085	1098
TRUE	41876	34846	31879	2967	6103	867

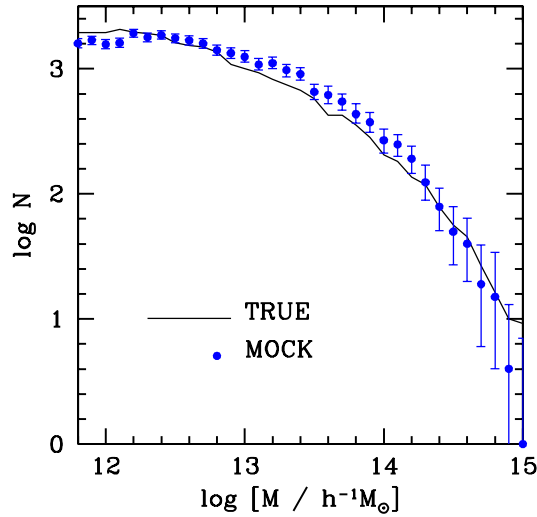


FIG. 9.— The halo mass function. The results obtained from the group catalog constructed from the mock galaxy sample are represented by solid points. The error bars are estimated from 1000 bootstrap re-samplings. The black solid curve represents the halo mass function obtained from TRUE halos in the mock 2MRS sample.

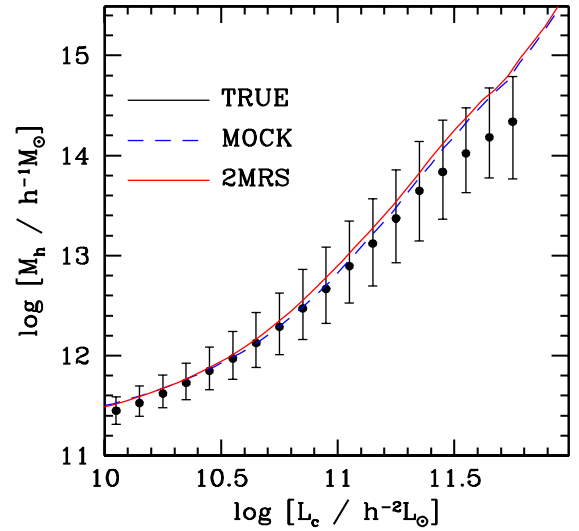


FIG. 10.— The final $L_c - M_h$ relation obtained from applying the modified halo-based group finder to 2MRS (red line). For comparison the final $L_c - M_h$ relation based on the MOCK sample is plotted with blue dashed curve. The black solid points with error bars represent the TRUE intrinsic $L_c - M_h$ relation in our mock 2MRS. The error bars indicate the 68% confidence level around the median.

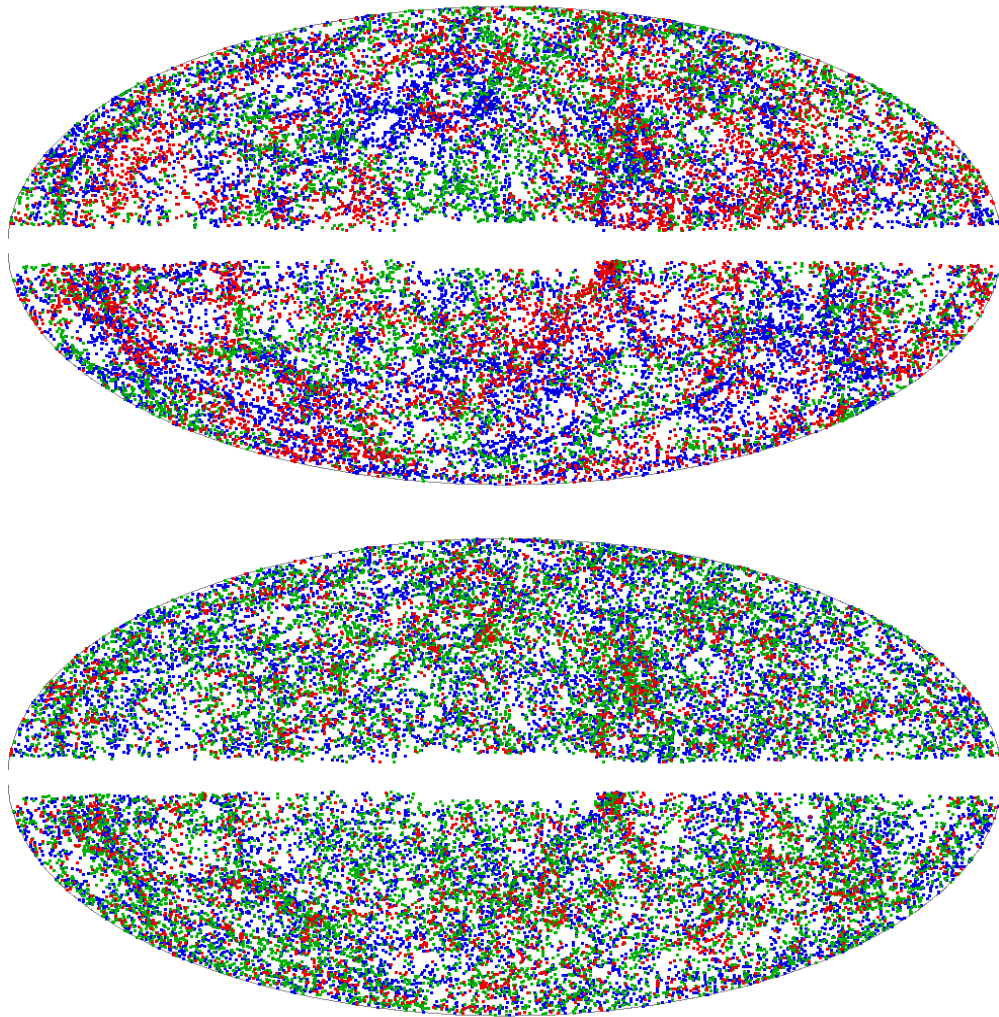


FIG. 11.— The distribution of 2MRS groups in Galactic coordinates, with Galactic longitude increasing from 0° at the center to 180° to the left, and from 180° from the right to 360° at the center. The Galactic latitude from -90° to 90° from bottom to top. Upper panel: red, green and blue points represent groups within the redshift range: $0.0 \leq z \leq 0.02$, $0.02 \leq z \leq 0.03$ and $0.03 \leq z \leq 0.08$, respectively. Lower panel: red, green and blue points represent groups within the mass range: $\log M_h \geq 13.5$, $13.5 \geq \log M_h \geq 12.5$ and $12.5 \geq \log M_h$, respectively.

are shown in the left and right panels of Fig. 12. The circles roughly correspond to the shell of our 2MRS sample at $z = 0.08$. The decline of the density from the center towards the edge is mainly caused by the survey selection effect, so that only massive groups are detected at large distances.

Table 3 lists the number of groups in the 2MRS within two redshift ranges: $z = 0.01 - 0.03$ and $z \leq 0.08$, with single member or with more than one member. We also list the number of massive groups with estimated halo masses in two mass ranges, $14.0 \geq \log M_h \geq 13.0$ and $\log M_h \geq 14.0$. For comparison, the number of the mock galaxy groups (MOCK) and halos (TRUE) in the redshift range $z \leq 0.08$ are also listed in Table 3. Overall, the 2MRS sample tends to contain more rich groups with $N > 32$ than in the mock, as shown in the left panel of Fig. 13. However, the total number of such rich systems is small and the statistic is rather poor. The middle panel of Fig. 13 shows the redshift distribution of groups, where the redshift of each group is the luminosity-weighted average of the redshifts of its member galaxies. Here we see that the 2MRS sample contains slightly less groups at low red-

shift and slightly more groups at high redshift than the mock 2MRS sample.

One of the purposes of constructing the 2MRS galaxy group catalog is to populate the local Universe with well estimated dark matter halos for our subsequent reconstructions of the local density field (e.g. Wang et al. 2014). We check the halo mass function of galaxy groups in the 2MRS volume which are shown in the right panel of Fig. 13 using black points with error bars. For comparison, the halo mass functions of groups constructed from the mock 2MRS sample are also plotted in this figure. Since we require both of the halo mass functions of MOCK and 2MRS to agree with the theoretical prediction, the agreement between the two is expected.

5.2. Comparisons with previous results

In a recent study, Tully (2015, hereafter T15) identified galaxy groups from the 2MRS using a modified version of the halo-based group finder developed by Yang et al. (2005a), with halo masses estimated from a scaling relation to the characteristic group luminosity. Tully identified 13,606 groups

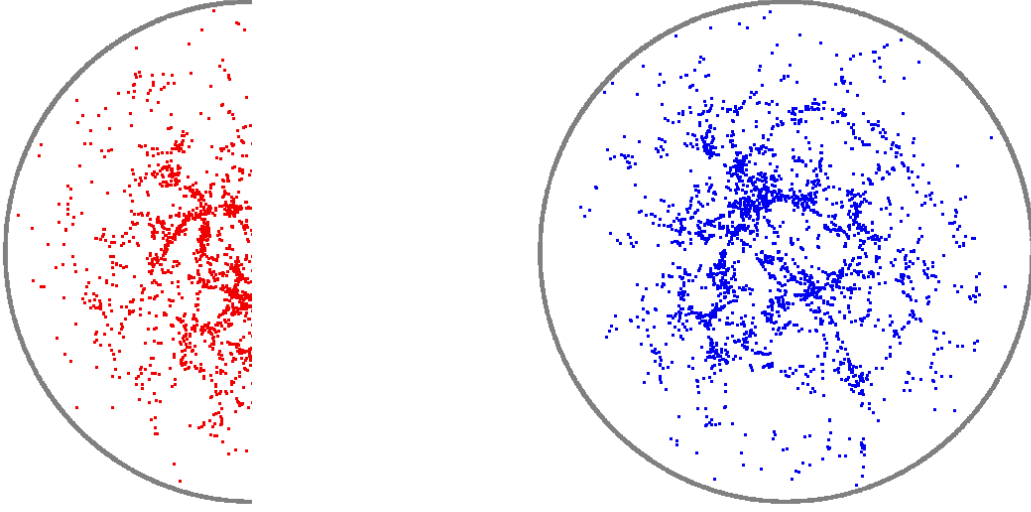


FIG. 12.— The distribution of 2MRS groups in two slices with $10 < b \leq 20$ (left panel) and $-20 \leq b < -10$ (right panel), respectively. Galactic longitude changes from zero at the top counter-clock-wisely, while distance increases linearly from 0 at the center to $z = 0.08$ on the outer circle.

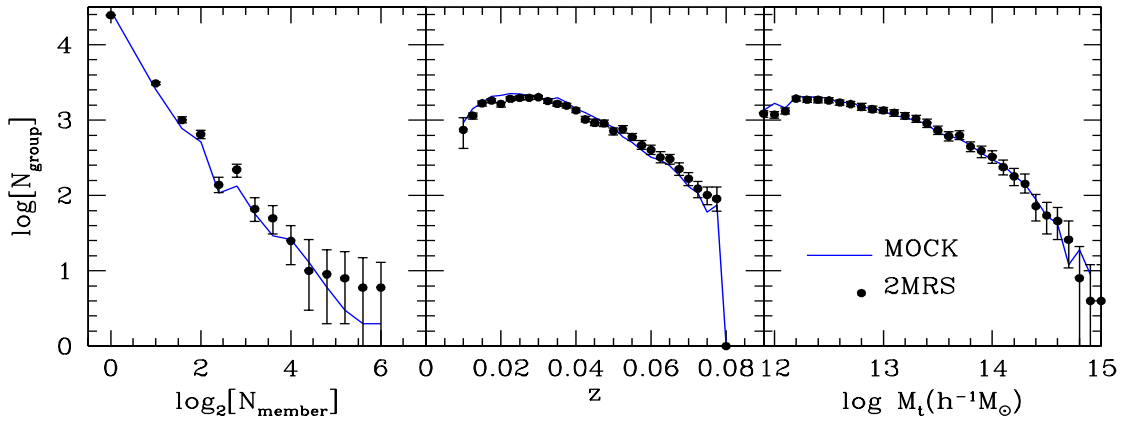


FIG. 13.— The number of groups as function of the number of group members (left panel), group redshift (middle panel) and halo mass (right panel). The solid points with error bars show the results obtained from the 2MRS group catalog constructed using the modified halo-based group finder. The error bars are given by 1000 bootstrap re-samplings. For comparison, in all panels, we also plot the corresponding distributions obtained from the mock 2MRS group catalog using curves.

TABLE 4
COMPARISON BETWEEN HALO MASSES (IN
 $\log[M_h / h^{-1} M_\odot]$)

Groups	Lu	T15	Literature
Abell2199	14.84	15.26	14.81 ¹
Coma	14.76	15.23	14.85 ²
Abell2634	14.59	14.90	14.61 ³
Perseus	14.59	15.07	
Norma	14.30	15.10	15.00 ⁴
Virgo	14.37	15.04	14.43-14.90 ⁵
Abell1367	14.34	14.80	

NOTE. — ¹ Kubo et al. (2009). ² Gavazzi et al. (2009). ³ Schindler & Prieto (1997). ⁴ Woudt et al. (2008). ⁵ Karachentsev & Nasonova (2010).

member. In comparison, our group catalog uses a different halo mass estimate and extends to a larger redshift range. In particular, we have used a realistic mock catalog to quantify the reliability of our group finder and the group masses it gives.

To compare with T15, we list in Table. 3 the properties of groups in the redshift range $0.01 \leq z \leq 0.03$, which is comparable to the redshift range used in T15. For a total of 20,921 galaxies, we identified 12,889 groups, which matches well the results of T15. The richest group has 184 member galaxies in our catalog, which is consistent with 180 member galaxies given by T15. Fig. 14 illustrates some groups we found in several regions, including groups in the Perseus-Pisces filament, Leo cluster, Norma cluster, Virgo and Coma clusters. We also list the estimated halo masses of some prominent nearby groups in Table. 4, in comparison to the results given by T15 for the same groups. In general, the halo masses given by T15 tend to be larger than the masses we obtain. We sus-

from a total 24,044 galaxies in the velocity range $3000 - 10,000 \text{ km s}^{-1}$, among which 3,461 have more than one

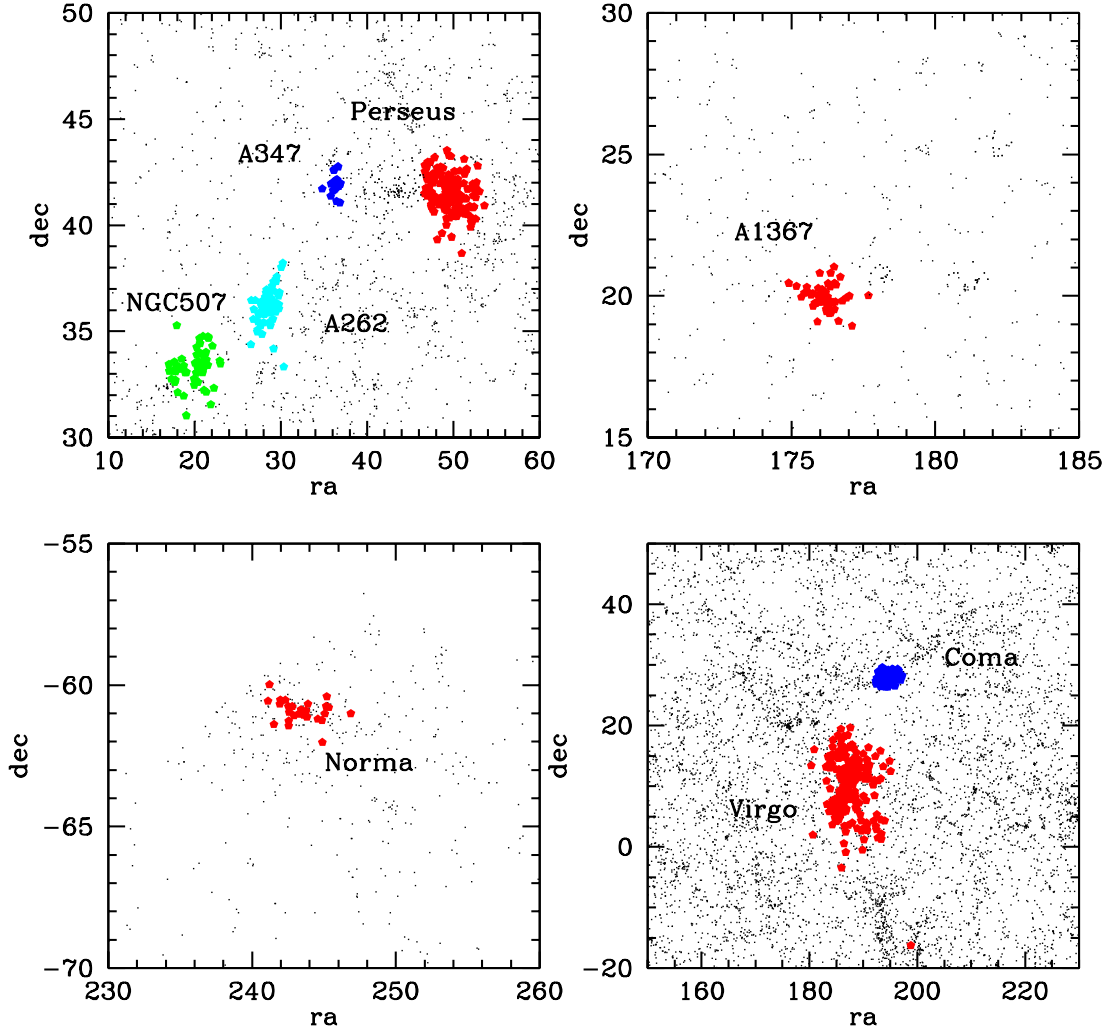


FIG. 14.— The Perseus-Pisces filament (top left), Leo Cluster (top right), Norma Cluster (bottom left) and Virgo Cluster (bottom right) given by the 2MRS group catalog.

pect that this is caused by different definitions of halo masses. To investigate this further, we looked into the literature for the halo masses of the groups in question, and the results are also shown in Table. 4. In general our mass estimates match well the values given in the literature. The only exception is the Norma cluster, for which our mass estimate is significantly lower. However, Norma is located near the Milky Way Zone of Avoidance, and is severely obscured by the interstellar dust at the optical wavelengths. It is unclear if this is also a significant problem in the near infrared data used here.

We further test our 2MRS group catalogs by comparing with an existing group catalog. This group catalog used here was constructed by Y07 from the New York University Value-Added Galaxy Catalog (Blanton et al. 2005, NYU-VAGC;) based on the SDSS Data Release 7. A total of 639,359 galaxies with redshifts $0.01 \leq z \leq 0.20$ and redshift completeness $C > 0.7$ were selected for constructing their group catalog. They found a total of 472,416 groups, among which 23,700 have three or more members. For our comparison,

we first cross match the 2MRS galaxies with the SDSS DR7 galaxies according to their coordinates in the sky. With the assumption that galaxies located within $5''$ of one another in the sky, and with a redshift difference of $\Delta z < 5 \times 10^{-4}$ (corresponding to a velocity of 150 km/s) are the same one, we got a total of 4,528 galaxy pairs, among which 2,938 galaxy pairs are centrals in both group catalogs.

We investigate the estimated halo masses assigned to the same halo in the two galaxy group catalogs. Here halos from the two group catalogs are matched if they have the same central galaxy according to the matched galaxy pairs. Note that, for the SDSS galaxy groups, the halo masses are estimated by the ‘RANK’ method, which estimates the halo mass of a candidate galaxy group according to its characteristic luminosity, $L_{-19.5}$, defined as the total luminosity of member galaxies brighter than a given luminosity threshold $0.1M_r - 5 \log h = -19.5$. The top panels in Fig. 15 show the estimated halo masses for all the 2,923 matched central galaxy pairs given by the 2MRS and SDSS DR7 group catalogs, re-

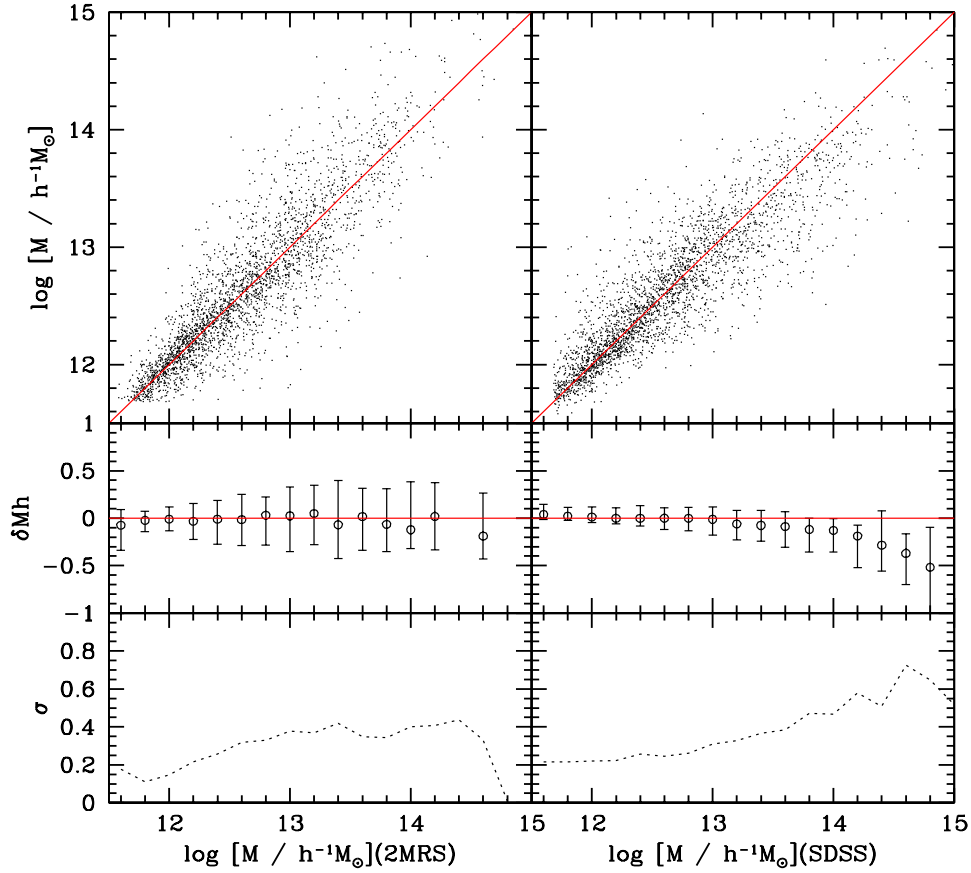


FIG. 15.— Comparison of the estimated halo mass between 2MRS and SDSS DR7 galaxy groups. This is similar to Fig. 8, but with the true halo masses replaced by SDSS DR7 halo masses. The difference between the two halo masses, $\delta M_h = \log M_{h2MRS} - \log M_{hSDSS}$ are also shown in the middle row in bins of halo mass obtained from the 2MRS (left) and SDSS (right), respectively. The error bars indicate 68% confidence level around the median. The standard variation of groups from the redlines in the top two panels are shown as the σ curves plotted in the bottom panels.

spectively. The top left and top right panels plot the same thing, except that the two mass axes are flipped: SDSS mass versus 2MRS mass in the left and 2MRS mass versus SDSS mass in the right). Ideally, the two estimated halo masses should be the same, so that all the data points would lie on the red solid line ($\log M_{h2MRS} = \log M_{hSDSS}$). We can see that the two halo masses estimated are tightly correlated with each other, with no obvious systematic bias (see the middle two panels which show the deviations from the perfect line). The typical scatter is ~ 0.4 dex in medium to massive halo mass range, and $\sim 0.2 - 0.3$ dex for low mass groups, as shown in the two lower panels. This scatter is roughly consistent with the one shown in Fig. 8 between the group and true halo masses estimated from the mock 2MRS catalogs.

6. SUMMARY

In this paper, we have implemented, tested and applied a modified version of the halo-based group finder developed in Yang et al. (2005a, 2007) to extract galaxy groups from the 2MRS. Covering uniformly about 91% of the sky, the 2MRS provides the best available representation of the structures in local universe, and so a group catalog constructed from it is useful for many purposes. However, 2MRS is quite shallow; in many cases only a few brightest members within a halo can be observed. To deal with this limit, we have updated the

halo mass estimate used in the previous group finder with a new method based on ‘GAP’. This ‘GAP’ estimator consists of two parts: (i) a relation between the luminosity of the central galaxy, L_c , and the halo mass, M_h , inferred iteratively from abundance matching between the luminosity of *central* galaxies and the masses of dark matter halos; (2) a luminosity gap correction factor obtained from the luminosity difference between the central galaxy and a faint satellite galaxy.

In order to evaluate the performance of our modified group finder, we have constructed mock 2MRS galaxy samples based on the observed K_s -band luminosity function. The group catalog obtained from the mock 2MRS galaxy catalog shows a 100% completeness for about 65% of the most massive groups to $\sim 85\%$ for groups with halo masses $\log M_h < 10^{14} h^{-1} M_{\odot}$. On average, about 80% of the groups have 80% completeness. In terms of interlopers, about 65% of the groups identified have none, and an additional 20% have an interloper fraction lower than 50%. Further tests on the halo mass estimation show that the deviation of the halo mass between the selected groups and the true halos is ~ 0.35 dex over the entire mass range. These tests demonstrate that the modified group finder is reliable for the 2MRS sample.

Applying the modified halo-based group finder to the 2MRS, we have obtained a group catalog with a depth to $z \leq 0.08$ and covering 91% of the whole sky. This 2MRS

group catalog contains a total of 29,904 groups, among which 24,618 are singles and 5,286 have more than one member. Some of the basic properties of the group catalog are presented, including the distributions in richness, in redshift and in halo mass. This catalog provides a useful data base to study galaxies in different environments. In particular, it can be used to reconstruct the mass distribution in the local Universe, as we will do in a forthcoming paper.

ACKNOWLEDGEMENTS

This work is supported by 973 Program (No. 2015CB857002), national science foundation of China

(grants Nos. 11203054, 11128306, 11121062, 11233005, 11073017), NCET-11-0879, the Strategic Priority Research Program “The Emergence of Cosmological Structures” of the Chinese Academy of Sciences, Grant No. XDB09000000 and the Shanghai Committee of Science and Technology, China (grant No. 12ZR1452800). We also thank the support of a key laboratory grant from the Office of Science and Technology, Shanghai Municipal Government (No. 11DZ2260700). HJM would like to acknowledge the support of NSF AST-1517528.

A computing facility award on the PI cluster at Shanghai Jiao Tong University is acknowledged. This work is also supported by the High Performance Computing Resource in the Core Facility for Advanced Research Computing at Shanghai Astronomical Observatory.

REFERENCES

- Behroozi, P. S., Conroy, C., & Wechsler, R. H. 2010, *ApJ*, 717, 379
- Berlind, A. A., & Weinberg, D. H. 2002, *ApJ*, 575, 587
- Berlind, A. A., Frieman, J., Weinberg, D. H., et al. 2006, *ApJS*, 167, 1
- Blanton, M. R., Schlegel, D. J., Strauss, M. A., et al. 2005, *AJ*, 129, 2562
- Bryan, G. L., Norman, M. L., Stone, J. M., Cen, R., & Ostriker, J. P. 1995, *Computer Physics Communications*, 89, 149
- Cacciato, M., van den Bosch, F. C., More, S., et al. 2009, *MNRAS*, 394, 929
- Conroy, C., Wechsler, R. H., & Kravtsov, A. V. 2006, *ApJ*, 647, 201
- Cooray, Asantha, 2006, *MNRAS*, 365, 842C
- Crook, A. C., Huchra, J. P., Martimbeau, N., et al. 2007, *ApJ*, 655, 790
- Croton, D. J., Springel, V., White, S. D. M., et al. 2006, *MNRAS*, 365, 11
- Davis, M., Efstathiou, G., Frenk, C. S., & White, S. D. M. 1985, *ApJ*, 292, 371
- Eke, V. R., Baugh, C. M., Cole, S., et al. 2004, *MNRAS*, 348, 866
- Erfanianfar, G., Popesso, P., Finoguenov, A., et al. 2014, *MNRAS*, 445, 2725
- Felten, J. E. 1976, *ApJ*, 207, 700
- Gavazzi, R., Adami, C., Durret, F., et al. 2009, *A&A*, 498, L33
- Guo, Q., White, S., Li, C., & Boylan-Kolchin, M. 2010, *MNRAS*, 404, 1111
- Hinshaw, G., Larson, D., Komatsu, E., et al. 2013, *ApJS*, 208, 19
- Huchra, J. P., & Geller, M. J. 1982, *ApJ*, 257, 423
- Huchra, J. P., Macri, L. M., Masters, K. L., et al. 2012, *ApJS*, 199, 26
- Jarrett, T. H., Chester, T., Cutri, R., et al. 2000, *AJ*, 119, 2498
- Jarrett, T. H., Chester, T., Cutri, R., Schneider, S. E., & Huchra, J. P. 2003, *AJ*, 125, 525
- Jiang, N., Wang, H., Mo, H., et al. 2016, *arXiv:1602.08825*
- Jing, Y. P., Mo, H. J., & Börner, G. 1998, *ApJ*, 494, 1
- Kang, X., Jing, Y. P., Mo, H. J., Börner, G. 2005, *ApJ*, 631, 21
- Karachentsev, I. D., Tully, R. B., Wu, P.-F., Shaya, E. J., & Dolphin, A. E. 2014, *ApJ*, 782, 4
- Karachentsev, I. D., Makarov, D. I., & Kaisina, E. I. 2013, *AJ*, 145, 101
- Karachentsev, I. D., & Nasonova, O. G. 2010, *MNRAS*, 405, 1075
- Karachentsev, I. D., & Makarov, D. A. 1996, *AJ*, 111, 794
- Kim, R. S. J., Kepner, J. V., Postman, M., et al. 2002, *AJ*, 123, 20
- Koester, B. P., McKay, T. A., Annis, J., et al. 2007, *ApJ*, 660, 221
- Kravtsov, A. V., Klypin, A., & Hoffman, Y. 2002, *ApJ*, 571, 563
- Kubo, J. M., Annis, J., Hardin, F. M., et al. 2009, *ApJ*, 702, L110
- Lan, T.-W., Ménard, B., & Mo, H. 2016, *MNRAS*, 456, 217
- Li, S., Zhang, Y., Yang, X., Wang, H., Tweed, D., Liu, C., Yang, L., Shi, F., Lu, Y., Luo, W., & Wei, J. 2016, *Research in Astronomy and Astrophysics*, **submitted**
- Lu, Z., Mo, H. J., Lu, Y., et al. 2015, *MNRAS*, 450, 1604
- Lu, Z., Mo, H. J., Lu, Y., et al. 2014, *MNRAS*, 439, 1294
- Lu, Y., Yang, X., & Shen, S. 2015, *ApJ*, 804, 55
- Mo, H. J., & White, S. D. M. 2002, *MNRAS*, 336, 112
- Mo, H. J., Mao, S., & White, S. D. M. 1999, *MNRAS*, 304, 175
- Navarro, J. F., Frenk, C. S., & White, S. D. M. 1997, *ApJ*, 490, 493
- Nurmi, P., Heinämäki, P., Sepp, T., et al. 2013, *MNRAS*, 436, 380
- Peacock, J. A., & Smith, R. E., 2000, *MNRAS*, 318, 1144P
- Rodríguez-Puebla, A., Avila-Reese, V., Yang, X., et al. 2015, *ApJ*, 799, 130
- Schechter, P. 1976, *ApJ*, 203, 297
- Schmidt, M. 1968, *ApJ*, 151, 393
- Schindler, S., & Prieto, M. A. 1997, *A&A*, 327, 37
- Springel, V., White, S. D. M., Jenkins, A., et al. 2005, *Nature*, 435, 629
- Springel, V. 2010, *MNRAS*, 401, 791
- Tago, E., Saar, E., Tempel, E., et al. 2010, *A&A*, 514, AA102
- Tal, T., Dekel, A., Oesch, P., et al. 2014, *ApJ*, 789, 164
- Teyssier, R. 2002, *A&A*, 385, 337
- Tinker, J. L. 2005, Ph.D. Thesis, 3180
- Tinker, J., Kravtsov, A. V., Klypin, A., et al. 2008, *ApJ*, 688, 709-728
- Trujillo-Gomez, S., Klypin, A., Primack, J., & Romanowsky, A. J. 2011, *ApJ*, 742, 16
- Tully, R. B. 2015, *AJ*, 149, 171
- Vale, A., & Ostriker, J. P. 2004, *MNRAS*, 353, 189
- Vale, A., & Ostriker, J. P. 2006, *MNRAS*, 371, 1173
- van den Bosch, F. C. 2002, *MNRAS*, 332, 456
- van den Bosch, F. C., Yang, X., & Mo, H. J. 2003, *MNRAS*, 340, 771
- van den Bosch, F. C., Yang, X., Mo, H. J., et al. 2007, *MNRAS*, 376, 841
- Wadsley, J. W., Stadel, J., & Quinn, T. 2004, *New Astronomy*, 9, 137
- Wang, H., Mo, H. J., Yang, X., & van den Bosch, F. C. 2012, *MNRAS*, 420, 1809
- Wang, H., Mo, H. J., Yang, X., & van den Bosch, F. C. 2013, *ApJ*, 772, 63
- Wang, H., Mo, H. J., Yang, X., Jing, Y. P., & Lin, W. P. 2014, *ApJ*, 794, 94
- Weinmann, S. M., van den Bosch, F. C., Yang, X., & Mo, H. J. 2006a, *MNRAS*, 366, 2
- Woudt, P. A., Kraan-Korteweg, R. C., Lucey, J., Fairall, A. P., & Moore, S. A. W. 2008, *MNRAS*, 383, 445
- Yan, R., Madgwick, D. S., & White, M. 2003, *ApJ*, 598, 848
- Yang, X., Mo, H. J., van den Bosch, F. C., 2003, *MNRAS*, 339, 1057Y
- Yang, X., Mo, H. J., Jing, Y. P., van den Bosch, F. C., & Chu, Y. 2004, *MNRAS*, 350, 1153
- Yang, X., Mo, H. J., van den Bosch, F. C., & Jing, Y. P. 2005a, *MNRAS*, 356, 1293
- Yang, X., Mo, H. J., Jing, Y. P., & van den Bosch, F. C. 2005b, *MNRAS*, 358, 217
- Yang, X., Mo, H. J., van den Bosch, F. C., et al. 2005c, *MNRAS*, 362, 711
- Yang, X., Mo, H. J., van den Bosch, F. C., et al. 2007, *ApJ*, 671, 153
- Yang, X., Mo, H. J., & van den Bosch, F. C. 2008, *ApJ*, 676, 248
- Yang, X., Mo, H. J., van den Bosch, F. C., Zhang, Y., & Han, J. 2012, *ApJ*, 752, 41
- Zheng, Z., Berlind, A. A., Weinberg, D. H., et al. 2005, *ApJ*, 633, 791